Turk J Phys
30 (2006) , 197 – 212.

Dimensional Crossover in Semiconductor Structures: From 3D Electron Transport to Ballistic Electrons in 1D

Karl-Fredrick BERGGREN
IFM, Linköping University, S-58183 Linköping-SWEDEN

Received 18.07.2006

Abstract

Modern semiconductor technologies have made possible special devices in which a gradual dimensional crossover may be induced by means of applied electric fields. Two specific examples are described. The first one is a special GaAs field effect transistor in which the thickness of the active electron gas layer may be varied by external voltages. With decreasing layer thickness transverse states become quantized and by depopulating the corresponding subbands a tunable dimensional crossover from 3D to 2D is achieved. The second example describes how a 2D to 1D crossover may be obtained in high-mobility split-gate GaAs/AlGaAs heterostructures. Effects of interactions in long wires, the nature of spontaneous magnetization and quantized conduction are discussed. Anomalous features in the conductance are modeled by means of the local spin density approximation for a realistic split-gate device. Advantages and disadvantages of this method are discussed.

1. Introduction

Thanks to advances in technology it is now possible to make semiconductor devices that are about as small as the wavelength of an electron (or hole). The motion of a carrier in such devices becomes quantized in one, two, or three dimensions depending on the geometric shape of the object. One may say that there is a "freeze out" of dimensions as free particle states turn into standing waves because of some confining potential being added or the shape of the object is changed. "Dimensionality" in this context refers to the number of degrees of freedom of electron momenta. An electron a in two-dimensional (2D) system, for example, has its momentum fixed in one direction and a one-dimensional system in two directions. This article is about how electrons in specially designed semiconductor devices may be manipulated in a controlled fashion such that "dimensional freeze out" is achieved. There is a rich physics associated with this development, to which Mehmet Tomak has made early [1, 2] as well as recent [3, 4] contributions.

Consider a large block of material of volume L^3, in which the electrons are free to travel in any directions as a plane wave with wave vector $\mathbf{k}$:

$$\Psi_{\mathbf{k}}(\mathbf{r}) = \exp(i\mathbf{k}\cdot\mathbf{r})/L^{3/2}. \tag{1}$$

It could be a piece of an alkali metal, for example, and the valence electrons may be viewed as a 3D free electron gas. If we now by some means, for example by cutting or metal deposition, create a thin slab so that the electrons can still travel freely in two directions, but their third direction will be restricted. A scenario of this kind may be created very elegantly by means of a semiconductor device. In an active n-region, let us say, the carriers are assumed to occupy the conduction band. Within the effective mass approximation we let the electron states be represented by plane wave states. Effectively we are thus dealing with an electron gas. By proper combinations of materials, doping profiles, patterned gates and applied gate voltages, for

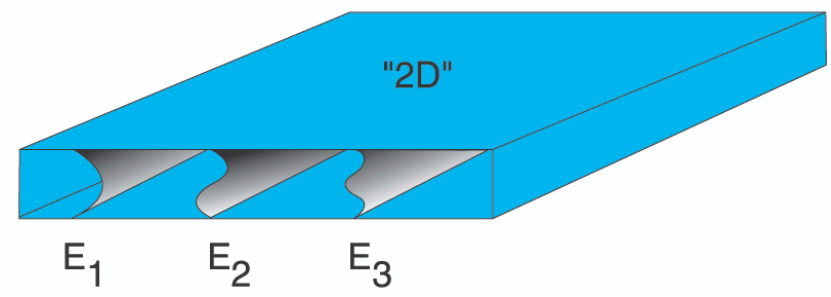

Figure 1. In a large 3D conductor electrons can travel freely in all directions and form a 3D electron gas. In a thin slab of the material, however, the motion of the electrons across the slab is quantized. The lowest three energies - E_1, E_2 and E_3 - are shown, along with the corresponding transverse wave function. The electrons can, however, travel freely in the plane of the slab. Symbols E_1, E_2 etc. refer to E_n^z in text. (Edited from Ref. [5].)

example, the electron gas may shaped in different fashions. It may flattened to a 2D system, elongated into a 1D wire, etc. in endless ways. This is the story to be told here.

The paper is organized in the following way. In Section 2 we describe what is meant by quasi-2D systems and a 3D to 2D transition. A realization of such a transition is discussed in Section 3 with a special GaAs-FET as a practical example. Section 4 outlines the basic properties of quasi-1D systems and an elementary derivation of quantized conductance is given. A real example of a quasi-1D system is given in Section 5 in terms of a split-gate device. Effects of interactions on electric transport and spontaneous magnetization are discussed in Section 6 for infinite ideal wires. Numerical modeling of realistic device structures by means of the local spin-density approximation (LSDA) are introduced in Section 7. Section 8, finally, contains a brief summary and concluding remarks.

2. Quasi-two-dimensional systems

Consider the slab in Figure 1 and assume that we deal with the ideal case of single electron states, i.e., we ignore for the moment electron interactions and scattering from impurities. The wave function for an electron occupying the nth transverse state in the slab is then

$$\Psi_{n,\mathbf{k}_{||}}(\mathbf{r}) = \phi_n(z)\exp(i\mathbf{k}_{||}\cdot\mathbf{r}_{||})/L\,, \tag{2}$$

with $\mathbf{r} = (x, y, z)$ and $\mathbf{r}_{||} = (x, y)$. The function $\phi_n(z)$ refers to the oscillatory motion between the walls and and $\exp(i\mathbf{k}_{||}\cdot\mathbf{r}_{||})/L$ to the free particle motion along the slab of size $L \times L$. The corresponding energy of the particle is therefore

$$E_n(\mathbf{k}_{||}) = E_n^z + \frac{\hbar^2 k_{||}^2}{2m^*}\,, \tag{3}$$

where E_n^z is the n'th quantized sublevel associated with the transverse motion in the z-direction as illustrated schematically in Figure 1. If the thickness of the slab is t we have $E_n^z = (n\pi\hbar)^2/(2m^*t^2)$ with $n = 1, 2, \ldots$ for hard wall confinement. In the remaining part of this section we simply write E_n without superscript z.

The density-of-states $N(E)$, which is continuous in 3D and depends on energy as $\sqrt{E}$, is now split up into discrete steps corresponding to the different transverse sublevels. The density-of-states is therefore for the two spin directions is

$$N(E) = \sum_n \frac{m^*}{\pi\hbar^2}\Theta(E - E_n), \tag{4}$$

where $\Theta(x)$ is a step function (see Figure 2). When only the lowest subband is occupied, as in Figure 2, the system is effectively two-dimensional. In the limit of large number of occupied levels the system turns 3D. In practice this happens rather rapidly, let us say $n > 10$.

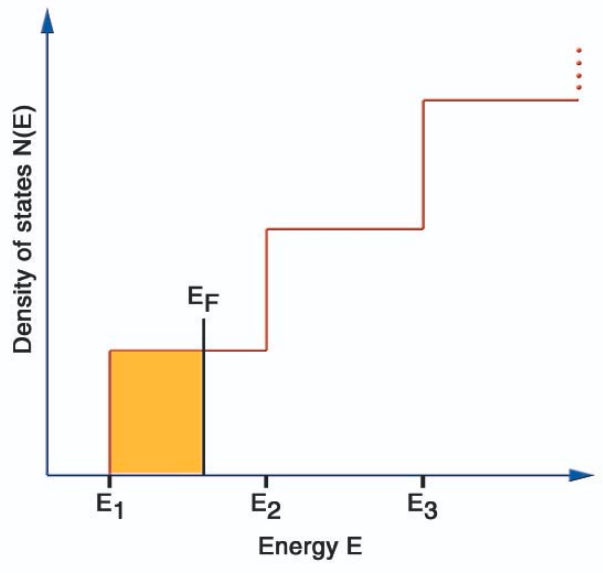

Figure 2. In a slab the density-of-states, $N(E)$, increases increases step-like as a function of energy, E. The figure shows the case when only the lowest subband is occupied, i.e., the Fermi energy $E_F < E_2$. The system is then in practice two-dimensional. (Edited from Ref. [5].)

3. Realization of a quasi-two-dimensional system

The question is how to achieve a transition from 3D to 2D behavior in practice. One way is to fabricate thin solid films which are thin enough to display quantum size effects (QSE). This approach is well established since long [6]. The first observation of QSE was made for bismuth films [7] already in 1966. As mentioned in the introduction modern semiconductor technology offers flexible alternatives to this somewhat tedious way. An early example [8] in this development is shown in Figure 3. In this versatile special GaAs field-effect transistor (FET) the electrons occupying the conduction band in the n-doped region form a metallic state when the doping concentration is chosen to be above the the Mott critical concentration. Because of the depletion layers the electrons thus form an electron gas in the shape of a slab as in Figure 1. The thickness may be varied elegantly by means of the gate and substrate voltages. A transition from 3D to 2D was inferred from measurements of the Shubnikov-de Haas oscillations and semi-classical modeling of the transverse quantized sublevels $E_1, E_2, E_3, ...$ in the metallic slab as in Figure 1 [8].

In an early paper dealing with the dimensionality of the special GaAs-FET Tomak et al. [1] showed that the plasmon dispersions indeed display 2D behavior as sublevels gradually become depopulated. In a subsequent paper the dc electrical transport properties were studied as function of layer thickness t [2]. Using the Boltzmann transport equation modified to the case of multi-subbands the sheet resistance was evaluated using real device characteristics for the special GaAs-FET. The scatterers, in this case the ionized donors in the n-doped region, were included as dielectrically screened point charges.

The numerical simulations by Tomak and coworkers [2] did indeed predict a transition from 3D to 2D transport with decreasing t. The sheet resistance was found to increase with pronounced steps each time the Fermi energy E_F passes a sublevel E_n, which appears consistent with the step-like behavior of the density-of-states in Figure 2. The detailed agreement between theory and experiments were, however, rather modest. There was an overall similarity between theory and measurements in the sense that the sheet resistance did increase with decreasing layer thickness t, but the predicted structure associated with the depopulation of sublevels was not observed. The reason for this discrepancy may be understood in the following way. The conduction takes place amidst the ionized donors. Scattering effects are therefore strong, presumably much stronger than the single scattering events that were included in the Boltzmann transport equation [2]. The strong scattering evidently introduces broadening effects and for this reason the predicted structure in the sheet resistance was not confirmed by experiments.

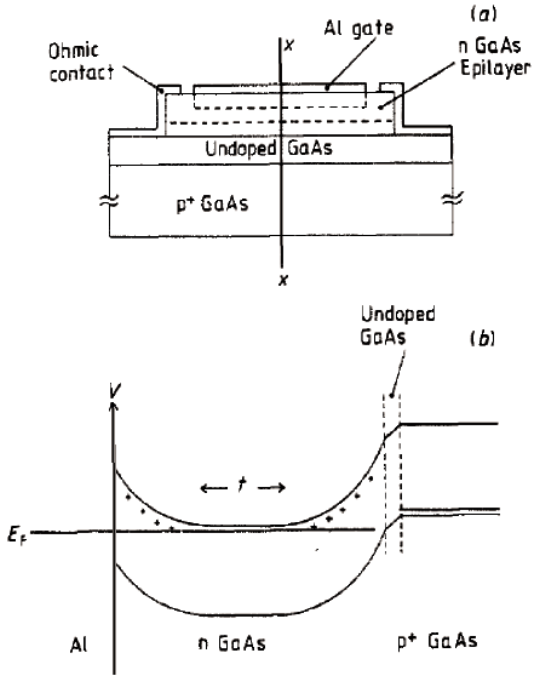

Figure 3. (a) shows schematically the cross sectional view of a special GaAs FET device with a controllable n-doped conducting region (epilayer). The thickness, t, and position of the conducting region/slab may by varied by applied gate and substrate voltages. (b) illustrates the potential energy diagram along the x-direction in (a). The electrons are confined to the middle flat region of width t by the depletion regions on the two sides. If t is made to decrease by the applied voltages the transverse motion in the slab becomes quantized and the corresponding subbands gradually depopulate until only the lowest subband is occupied (from Ref. [8]).

A way out of the above dilemma is, of course, to use a device with much higher mobility, ideally a ballistic device. Modulation-doped semiconductor heterostructures offer such possibilities. In these systems electrons are transferred from the doping region to the interface where they form a lateral high-mobility electron gas. Depending on the electron density/perpendicular confinement one or more subbands are occupied. In the $In_{0.83}Ga_{0.47}As/In_{0.52}Al_{0.48}As$ heterojunctions studied in [9] more than one 2D subband was occupied. The measured magnetoresistance showed increase and subsequent drops with increasing magnetic field which is consistent with depopulation of 2D subbands and the behavior predicted by Tomak and co-workers [2]. However, the experimental data indicate that the importance of lifetime broadening of subbands even in these high-mobility systems. In the next section we will therefore discuss how dimensionality may be reduced further and how ultra-small quasi-1D semiconductor devices may be fabricated from gated heterojunctions. Because of the small size, typically less than the 2D elastic mean free path, the transport through a device turns ballistic. As a consequence broadening effects due scattering from imperfections are minimized.

4. Quasi-one-dimensional systems

For qualitative discussion of the basic properties of quasi-1D systems, let us first return to the slab in Figure 1. Obviously, the dimensionality of our model system of non-interacting electrons may be reduced further by cutting a thin stripe or wire out of the slab. A particle can still propagate freely along the straight wire, let this be the x-direction, while the transverse motion in the y-direction becomes quantized in addition to the z-motion of previous section. Assume for simplicity that the cross section is rectangular with height t and width w. The wave function may then be written as

$$\Psi_{n,m,k}(\mathbf{r}) = \varphi_n(y)\phi_m(z)\exp(ikx)/\sqrt{L}. \tag{5}$$

The functions $\varphi_n(y)$ and $\phi_m(z)$ refer to the oscillatory motion between the walls and $\exp(ikx)/\sqrt{L}$ to the free particle motion along the wire.

To evaluate the conductance of a wire let us first consider simple case of a strictly 1D case, i.e., we ignore for the moment the two transverse modes $\phi_n(z)$ and $\varphi_m(y)$ in Eq. (5). The wave function then reduces to the plane wave state $\exp(ikx)/\sqrt{L}$ with energy $E(k) = \hbar^2k^2/2m^*$. Let us separate the density-of-state as $N(E) = N_+(E) + N_-(E)$ where $(+,-)$ refers to states propagating in the two opposite directions with $k > 0$ and $k < 0$. The partial density-of-states per spin is then

$$N_{+,-}(E) = \pm\frac{1}{2\pi}\left(\frac{dE}{dk}\right)^{-1} = \pm\frac{m^*}{2\pi\hbar^2k} = \frac{1}{4\pi\hbar}\sqrt{\frac{2m^*}{E}}. \tag{6}$$

The velocity is $v_x = \hbar k/m^*$. If there is a voltage drop V between the two ends of the $1D$ wire a net current will flow in, let us say, the positive $x-$direction. The current $I(V)$ then derives derives from states with $k > 0$ within an energy window $(E_F - eV/2, E_F + eV/2)$. Assuming zero temperature we thus obtain

$$I(V) = \int_{E_F-eV/2}^{E_F+eV/2} N_+(E)(ev_x)dE = (e^2/h)V \tag{7}$$

where E_F is the Fermi energy. The conductance per spin direction is therefore $G = I/V = e^2/h$ and for the two spin directions $G = 2e^2/h$.

To generalize the results for the ideal 1D case to a real wire we have to include the transverse motions in the y and z directions.

$$E_{n,m}(k) = \hbar^2k^2/2m^* + E_n^y + E_m^z, \tag{8}$$

with $E_n^y = (n\pi\hbar)^2/(2m^*w^2)$ in analogy with E_m^z above. Assume now that the cross sectional width w is much larger than the thickness t. We also assume that $E_1^z < E_F < E_2^z$. In this case we limit our discussion to the sublevels E_n^y since E_1^z will only serve as a reference energy. We will therefore omit E_m^z from the following expressions and simply write E_n for E_n^y. The total density of states for this multi-subband situation is therefore

$$N(E) = \sum_n \frac{1}{\pi\hbar}\sqrt{\frac{2m^*}{E - E_n}}\,\Theta(E - E_n), \tag{9}$$

which is shown schematically in Figure 4 with its characteristic square-root singularities at the sublevels E_n. When only the lowest subband is occupied as in Figure 4 the wire is effectively 1D. As higher subbands become populated, for example, by increasing the width w, there will be a gradual crossover to the initial 2D slab. Broadening due to scattering should make this process smooth in the limit of many occupied subbands (cf. previous section).

We may now derive the conductance in the same way as above. Each occupied subband contributes $(2e^2/h)$ to G, i.e., if there are N occupied levels we have the fundamental result

$$G = N(2e^2/h), \tag{10}$$

or with spin directions separated

$$G = (N_\uparrow + N_\downarrow)(e^2/h), \tag{11}$$

where $N_\uparrow$ and $N_\downarrow$ are the number of occupied up- and down-spin states, respectively. In the case of double occupancy the conductance would evidently change by $(2e^2/h)$ as the Fermi energy is made to pass a sublevel E_n. If the subbands are spin split by, for example, an external magnetic field the conductance step would be (e^2/h). These arguments imply that the transmission coefficient $T_n(E)$ for state n is a step function with values 0 or 1. A weakness of the model is, however, that we do not tell how the wire is contacted. Below we will find that this is an important point.

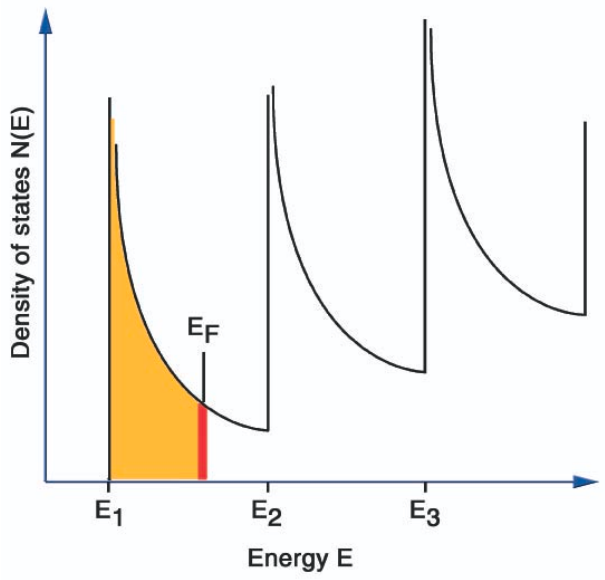

Figure 4. The density-of-states, $N(E)$, for a wire as a function of energy, E. The system is effectively one-dimensional when the electrons occupy only the lowest subband as in the figure. The narrow region, $\Delta = |eV|$, around the Fermi energy, E_F, indicates which states contribute to the net current. Below this region equal number of electrons flow in both directions, which means that they contribute zero net current. (Edited from Ref. [5].)

5. Realization of a quasi-one-dimensional system

There are many ways to fabricate narrow metallic wires. To stay with semiconductor materials we will, however, extend the ideas discussed above. Narrow channels may thus be achieved in practice by extending the principle design in Figure 3, which is based on a particular electrostatic confinement in the gated semiconductor structure. A first important step is to use modulation-doped GaAs/$Al_xGa_{1-x}As$ heterojunctions in which a 2D electron gas (2DEG) is formed at at the interface. Because the electrons and ionized donors are are spatially separated from each other the impurity scattering is drastically reduced resulting in exceedingly high mobilities (at low temperatures). This is evidently in contrast to the special GaAs-FET in Figure 3, in which the electrons and scattering centers reside in the same region.

A second important step is to use split gate techniques [10].[1] Figure 5 shows how a modulation-doped heterojunction may be gated selectively to achieve a narrow channel connecting two 2D reservoirs that serve as source and drain. By varying the applied voltages V_{sg} and V_g the electron density under the gated regions may be controlled. When these regions are depleted the remaining electrons are electrostatically confined to the ungated regions. Within the channel region the transverse motion will be quantized. If the lateral confinement is weak the separation between sublevels will be small. As a consequence, a large number of the subbands will be occupied. On the other hand, at stronger confinement (narrower channel) only a small number of subbands are occupied, eventually only the lowest. Thus one achieves a 2D to 1D dimensional crossover by simply varying a gate voltage.

The elementary considerations in previous section for non-interacting electrons tell that the conduction G for ideal long channels is quantized in units of $(2e^2/h)$. The conduction steps are sharp because the transmission coefficients are either zero or one. The conduction plateaux in G is experimentally well established [16, 17]. We recall at this point that the technological background to this remarkable experimental result is the availability of high-mobility modulation-doped materials with mean free-paths exceeding the length of the channel allowing for ballistic transport.

Figure 6 shows typical experimental data for G for a high-quality split gate device [18] with fifteen

[1]Here we focus on the split gate technique as quasi-1D was pioneered in this way. There are also other ways of fabricating narrow constrictions, e.g., by means of shallow etching [11], cleaved-edge overgrowth [12], and erasable electrostatic lithography (EEL) [13, 14].

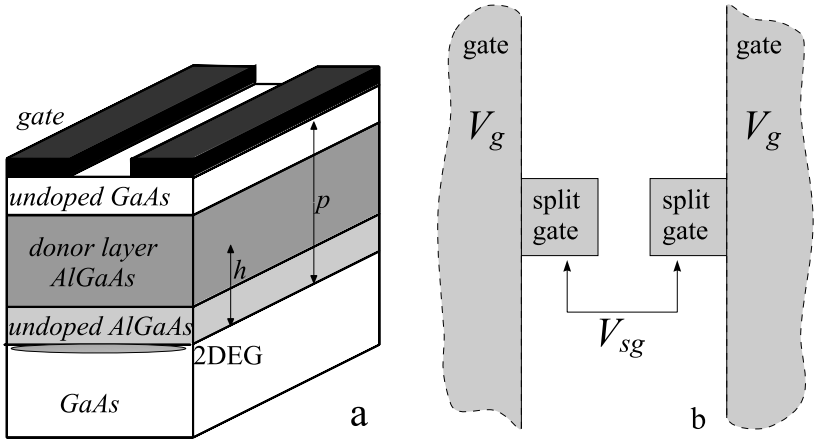

Figure 5. a) Schematic view of a modulation-doped GaAs/$Al_xGa_{1-x}As$ heterostructure with a split metallic gate. A 2D electron gas (2DEG) is formed at the interface. b) Top view of the gate showing a narrow split gate area that induces a narrow channel at the GaAs/AlGaAs interface. Upper and lower ungated areas indicate 2DEG reservoirs that serve as source and drain. To operate the device two voltages V_g and V_{sg} are applied separately to the gated regions; V_g and V_{sg} regulate the effective width and electron density of the reservoirs and the channel, respectively. An electric current flows through the QPC when a voltage difference V between source and drain is set up. (Re-edited from Ref. [15])

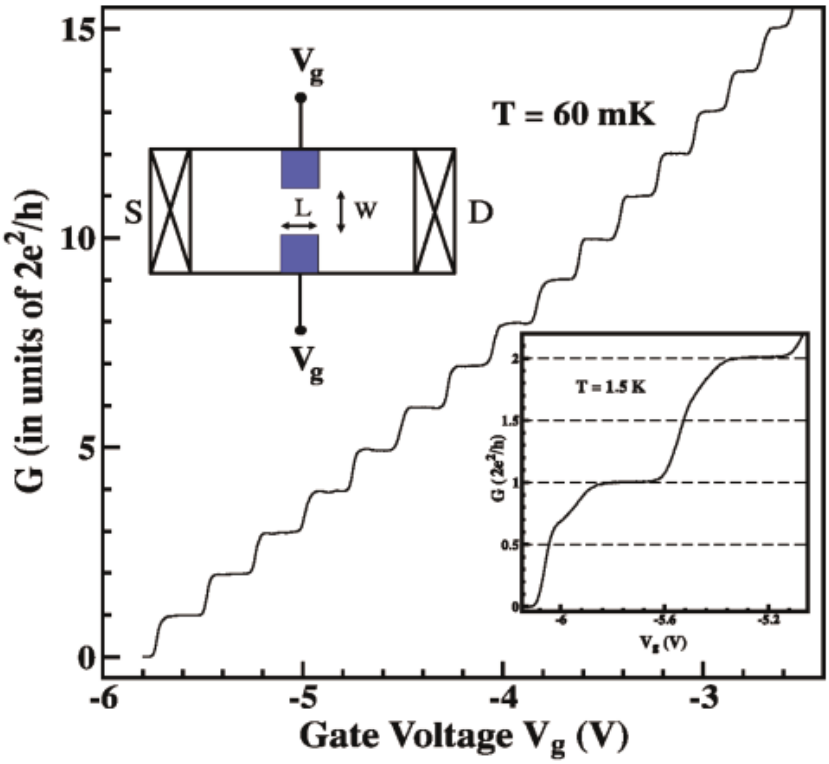

Figure 6. Measured conductance G at $T = 60$ mK as function of gate voltage for a QPC fabricated from high-mobility GaAs/$Al_xGa_{1-x}As$. The upper inset is a schematic view of the split gate device used in measurements; S and D represent the source and drain contacts. The lithographic length of the split gate is width is $L = 0.4$ μm and the width typically $W = 0.75 - 0.95$ μm. The lower inset shows a the first and second conduction plateaux at $T = 1.5$ K (Edited from Ref. [18]; courtesy M. Pepper and K.J. Thomas)

quantized plateaus clearly visible. Typical sublevel spacings for this kind of quantum devices are $\Delta E \sim 0.5-2$ meV. The simple theory in previous section is evidently consistent with the quantization of G. There are some important differences that we shall return to below. The step-like changes in G are not abrupt as expected from the discussion above. Instead there are smooth crossover region between the plateaux. Secondly there is an unusual feature associated with the lowest plateau, usually referred to as the "0.7 anomaly" [19]. The value 0.7 might give the impression that it might be a universal. Later studies have demonstrated, however, that the anomaly may occur at different conductance values depending on geometry and fabrication techniques (see e.g. [20, 21, 22]). Even dual structures have been reported recently [14]. In spite of this, one often talks about the phenomenon as the 0.7 conduction anomaly or structure for historic reasons and convenience. The details of this will be discussed in the following sections.

6. Effects of interactions in ideal wires

Since Thomas et al. [19] first draw attention to the 0.7 conduction anomaly in 1996 it has attracted great theoretical and experimental attention over the years as outlined in [5, 23, 24]. The dependence on magnetic field points to the importance of spin interactions. For example, with an increasing magnetic field the anomalous structure gradually turns into a 0.5 conduction plateau, the value expected for spin-split subbands as discussed above for an infinite channel. A most intriguing feature is the temperature dependence of the 0.7 conduction anomaly, which becomes more sharp with increasing temperature [11, 19].

The quantized conduction in Figure 6 is commonly presented in the literature to be a consequence of the 1D behavior quantum wires as discussed above. Not surprisingly much of the theoretical modeling has focused on infinite or very long wires that are quasi-1D in practice. Thus an explanation of the 0.7 anomaly, based on spontaneous spin polarization even in the absence of a magnetic field, was suggested in [25] using the local spin-density functional theory (LSDA) to include exchange interactions. Subbands were found to spin split as the Fermi energy was made to pass a subband threshold. The spin-ordering turned out to be ferromagnetic with an abrupt onset. On further increase of E_F the spin-gap will close, also in this case in an abrupt way. The abrupt reordering of spins has been elaborated more recently in connection with 0.7 variants which occur at the crossings of Zeeman-split subbands at high parallel magnetic field [26]. In this case theory based on LSDA is in accord with measurements [27].

The mechanism of spontaneous spin-splitting was developed further by Reilly et al. [28, 29, 30] by means of a phenomenological model. A density-dependent spin-gap is assumed to open in the 1D energy spectrum as the gate as above, but the density dependence is assumed to be linear. The closing of the gap on further increase of the density is not included in the model. Figure 7 shows schematically how the spin-gap is assumed to take place. Transmission coefficients are assumed to be either zero or one. In this sense the model thus refers to infinite or very long wires according to the dicussion above.

The phenomenological model is in good agreement with the experimental data for ultra-low-disorder quantum wires of length $L = 1$ μm and for the temperature range reported. In the same way the model is useful when analysing transport at finite source-drain bias.

Effects of electron interactions have also been studied by Taş and Tomak [3, 4, 31] who considered electrons occupying the lowest subband in an infinite harmonic wire. Using dielectric response theories a Bloch instability towards a ferromagnetic state was predicted to occur at low electron densities. This problem was also studied in Ref. [32]. Similar studies based on LSDA and response theory confirm the existence of ferromagnetic ordering [33]. An interesting aspect is that LSDA in combination with linear response theory yields a renormalized conductance for the magnetized state that is related to the compressibility as

$$G = (e^2/h)\sqrt{K/K_0}, \tag{12}$$

where K and K_0 are the compressibilities for interacting and non-interacting electrons, respectively. Depending on electron density the conductance then ranges from $\sim 0.5(e^2/h)$ to $\sim 0.7(2e^2/h)$. For the paramagnetic state the conductance is close to $(2e^2/h)$. Thus there are a number of theoretical investigations of ideal wires that predict that a spontaneous transition towards a ferromagnetically ordered state occurs at low subband filling. The different models predict a linear as well an abrupt onset as a function of electron density. However, there are objections in the literature [23, 24] to the existence of a spin-polarized ground state in

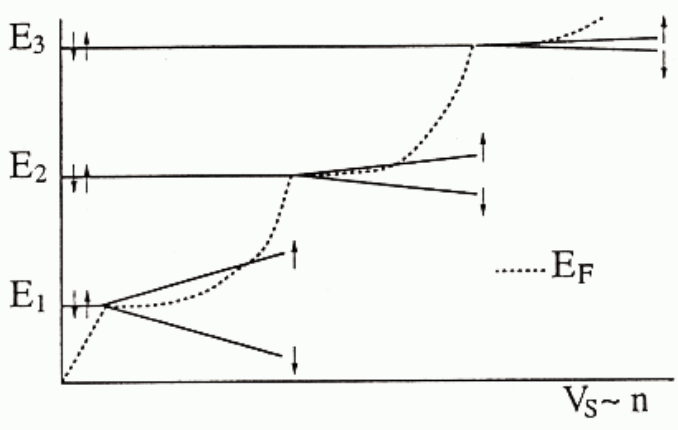

Figure 7. Phenomenological picture of a density-dependent spin-gap opening linearly with increasing density n or gate voltage (V_S). E_1, E_2, E_3 indicate the subband thresholds as above. The Fermi level (dashed line) is nonlinear with density n due to the singularities in the density-of-states in Eq. (4) (from Ref. [28]).

low-density quantum wires because of the Lieb-Mattis theorem [34]. According to this theorem the ground state of N electrons in strictly 1D subject to an arbitrary symmetric potential must be unmagnetized, or paramagnetic. As Taş and Tomak [3] point out, however, the theorem does not apply to the present case because electrons interact via 3D Coulomb potentials. In other words, our wires are not 1D in a mathematical sense because they have a finite cross section.

The cases above all favor ferromagnetic ordering. In principle there could also be other states induced by the interactions like various anti-ferromagnetic and spin-density wave states, ordered Wigner crystals etc. Obviously, states of this kind might be relevant for an explanation of 0.7 conduction anomaly. It is therefore interesting that Reimann and coworkers [35, 36] report on LSDA studies of a "spin-Peierls" transition for three different examples: "infinite" quasi-1D wires with periodic boundary conditions, quantum rings with a finite number of particles and straight wires of finite length, all three cases in the one-subband regime. A variety of states were found in this way. The infinite wire was modeled by a rectangular calculation box with periodic boundary. The detailed nature of the wire cross section was found essential for the occurrence of the spin-Peierls transition. Self-consistent LSDA yielded either an antiferromagnetic spin-density wave or paramagnetic solutions. For low densities and narrow wires the ground state was found to be a sinusoidal spin-density wave accompanied by a band gap at the Fermi level as expected for a Peierls transition. The Bloch transition to a polarized phase was found to occur for much narrower wires than for the SDW state. Antiferromagnetic solutions were also found for harmonic rings referred to as "spin Wigner molecules". Finally straight wires with finite length were simulated by means of needle-shaped anisotropic harmonic confinements. In this case the fully polarized states were found to be lower in energy than the antiferromagnetic SDW. The possibility of different states in a harmonic infinite wire are also discussed in [37, 38], in particlar Wigner and "zig-zag" electron lattices induced by electron interactions at low densities.

The studies of Reimann et al. [35, 36] are most relevant in the present context because they point to a number of possible states. For example, the fact that the SDW state is accompanied by a gap at the Fermi level is intriguing as it might be associated with the anomalous temperature dependence of the 0.7 conduction anomaly. Evidently geometry and electron densities matter. Therefore it is not immediately clear how the results for the above model systems may be applied to quantum wires and quantum point contacts in real modulation-doped split-gate GaAs/AlGaAs devices. In particular we note that theory does not tell how the electrons are injected and emitted, i.e., the role of leads or reservoirs. In this context we may recall the transport properties of a clean strictly 1D Luttinger liquid and the influence of leads. The dc conductance per spin is predicted to be Ke^2/h per spin direction if leads are disregarded; K is an interaction-dependent parameter characterizing the Luttinger liquid. For non-interacting electrons $K = 1$, but for repulsive interactions $K < 1$, and the conduction should be reduced. It has become clear, however, that the conductance is not renormalized by the electron interactions when the reservoirs (leads) are properly

taken into account [39]. Once more this calls for a type of modeling that includes leads, reservoirs, gating etc. In the next section we will therefore outline the results for realistic split-gate devices using LSDA.

7. LSDA modeling of realistic split-gate devices

As shown above the presence of quantized conduction plateaux $N(2e^2/h)$ in Figure 6 are easily explained in terms of non-interacting electrons in infinite wires, albeit we do not specify how the wires are contacted electrically. Hence the transmission coefficients $T_n(E)$ are either zero or one and, as a consequence, the steps in G must be abrupt, at least at lowest temperatures. Experiments show, however, that there is a smooth crossover between the different plateaux. Because the channels in a real device are of finite length tunneling will take place. In addition, the potential is not constant in the channel region but more like a saddle, as for example, the parabolic saddle potential

$$V(x,y) = V_0 - \frac{1}{2}m^*\omega_x^2 x^2 + \frac{1}{2}m^*\omega_y^2 y^2. \tag{13}$$

Here ω_x and ω_y are related to the curvatures of the potentials in the x- and y-directions and V_0 is the potential at the saddle maximum. The parabolic saddle potential accounts well for the normal integer quantized conductance in a QPCs on a one-electron level. It also accounts well for the gross features of the soft intermediate regions because it allows for tunneling [40]. Typical values for ω_x and ω_y are in the range $\sim$1 - 3 meV as obtained from bias spectroscopy [41]. An interesting question arises here. The saddle potential appears to be a better representation of the true potential in a typical split-gate QPC (short wire) device. One should therefore ask if it makes sense to refer to such a device, as frequently done, as a one-dimensional object. At this point one should also ask what is indeed meant by one-dimensionality in a strict sense. For example, if truly 1D the density of states should be as in Eq. (6). Depending on the ratio ω_x/ω_y the local density states may deviate considerably from the Eqs. (6) and (9) as discussed in [42]. As a consequence, criticism claiming that the Lieb-Mattis theorem [34] forbids spontaneous magnetization in our type of systems is not valid.

7.1. Spontaneous Spin Polarization

The simple saddle potential in Eq. (13) is obviously successful in many respects. However, it is a single particle model and therefore unable to cope with interaction effects, for example, the 0.7 conduction anomaly. There are a number of different approaches to deal with interactions. We have already mentioned LSDA, which was first applied to a parabolic wire with a short constriction in Ref. [43]. It readily predicted a local spontaneous magnetization within the constriction and a conduction plateau at 0.5. The reason that this actual value is too low is that only the exchange potential was included in the LSDA. It is known that exchange interactions tend to overdo magnetization, while Coulomb interactions usually are counteractive. The LSDA approach and related mean-field approaches for QPCs and wires in between reservoirs were further investigated in [15, 44–50] with the full exchange-correlation potential included in case of LSDA. These theories are successful in predicting conduction anomalies at 0.7 and nearby values as observed in experiments. Under certain conditions a value of 0.5 is found. Anomalies associated with local spontaneous spin polarization are also found in higher subbands [15]. Consequently, the results of LSDA and similar mean-field modeling are consistent with the original ideas about spin polarization [18, 19] and recent direct observations based on a special spin separation technique for a hole gas [51]. Strong evidence for complete spontaneous spin polarization has been found recently from source-drain energy-spectroscopy and tempertature response in a GaAs device in which the potential landscape is tuned to be symmetric [14].

7.2. Kondo-like behavior and ZBA

Evidently the formation of local magnetic moments in QPCs and wires is an important ingredient of the 0.7 story and LSDA and similar mean-field theories are successful in predicting such moments. At low temperatures there are, however, important aspects that this kind of theories cannot handle, i.e., the zero bias anomaly (ZBA) and the associated anomalous temperature dependence [52] (see also [23, 24]).

Lindelof [53] was the first one to draw attention to the similarity with the Kondo problem, who identified an activation energy, a "Kondo" temperature, and formulated a phenomenological theory based on a non-conducting bound state. The Kondo-like model was also developed in more detail by Meir al. [45]. Their model accounts quite well for the observed low temperature dependence of G. The Kondo-like scenario is also elaborated in Ref. [54] for an idealized 1D channel with distinct resonances. However, the explanations of the 0.7 conduction anomaly and the associated ZBA, based on Kondo-like mechanisms, have the drawback that they rely on the existence of discrete bound states, which is somewhat counterintuitive for open systems like ours. It has not yet been clearly explained how bound states or sharp resonances may arise inside a smooth constriction with realistic device parameters [15, 50]. Recently doubts about a Kondo-like mechanism have been raised on experimental grounds by Rokhinson et al. [51] and Graham et al. [55]. Besides the spin polarization and Kondo-type models there is at present a number of other scenarios for the 0.7 anomaly, e.g., the strictly 1D Luttinger model [56, 57].

7.3. LSDA modeling realistic devices

After the overview of the different scenarios for the 0.7 "mystery" we return to the modeling of realistic device structures. Much of the discussion in this section has relied on simplified model systems. However, when dealing with infinite wires in Section 6 we have stressed the importance of geometry including the nature of the coupling to the reservoirs. Thus subtle boundary effects and details in the potential landscape might give preference to a ferromagnetic rather than an anti-ferromagnetic state. In fact, an anti-ferromagnetic or spin-density wave state would indeed be welcome as it should be accompanied by an energy gap at the Fermi energy and thereby an activation energy.

With the above arguments we thus find it important to numerically simulate realistic devices as accurately as possible. In this way we gain confidence when comparing with measurements. However, there is also a price for this. The numerical work involved is more cumbersome and for this reason one should resort to effective and well established techniques. Because LSDA (and its spin restricted variant LDA) is known to work well for a wide range of problems in atomic, molecular, condensed matter physics and general micro- and nanoelectronic device engineering LSDA should be an obvious choice in the present context. The popularity of LSDA is in part because of its simplicity. The self-consistent equations for the different orbitals are mean-field like and therefore have the one-electron form

$$\left[-\frac{\hbar^2}{2m^*}\nabla^2 + U^\sigma_{eff}(x,y)\right]\psi^\sigma_i(x,y) = \varepsilon^\sigma_i \psi^\sigma_i(x,y), \tag{14}$$

The effective potential in (14) consists of electrostatic, Hartree, and exchange-correlation terms

$$U^\sigma_{eff}(x,y) = U_{conf}(x,y) + U_H(x,y) + U^\sigma_{xc}(x,y). \tag{15}$$

Here (x, y) refer the GaAs/AlGaAs in interface in Figure 5, let us say. The electrostatic confinement potential can in turn be written as a sum of different contributions from the patterned gate, donor and surface states, applied voltages etc. We refer to [15, 50] for the detailed expressions.

Because the orbitals $\psi^\sigma_i(x,y)$ depend on electron spin σ the possibility of spontaneous spin-ordering is already inherent in the spin-relaxed LSDA. The self-consistency will in principle yield the state with lowest energy. This state could be ferromagnetic, anti-ferromagnetic, it could be a spin-density wave state, Wigner lattice, "zig-zag" states, etc.

The LSDA equations have been solved for the device in Figure 5 for a wide range of voltages, length and width of the lithographic channel, etc. [15, 44, 50] and for varied initial input to the self-consistent procedure. The effective mass approximation is assumed throughout. Spontaneous spin-polarization is readily observed and the onset is accompanied by a conduction anomaly. Depending on the length of the constriction the value varies from 0.9 for very short constrictions to 0.5 for long ones. The dependence on length is in accord with experiments, although data for the very short gates are not yet available. In fact, the theory predicts that magnetization will not occur for very short split gates, but this remains to be verified experimentally. An interesting aspect is that the spin-ordering turns out to be ferromagnetic in all cases, in spite of extensive search for other states, in particular the antiferromagnetic state. Hence, we draw

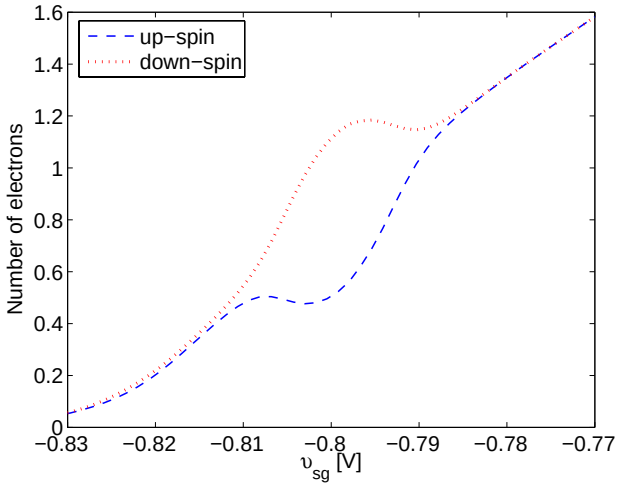

Figure 8. The number of up- and down-spin electrons in a 250 nm QPC as a function of the split split gate voltage. (From Ref. [50].)

the conclusion that, for the realistic device parameters, used here neither the formation of a Wigner crystal lattice nor an antiferromagnetic ground state is likely to take place.

The number of up- and down-spin electrons inside the constriction may be taken as a measure of the spin polarization. Figure 8 shows a typical example for which the conduction anomaly takes place at ~ 0.75. Evidently the features are smooth. For long channels the polarized region extends all the way down to pinch off. This means that the extra conduction plateau occurs at 0.5. For this value of the conduction and below the system is fully polarized. This may be of practical value as the system could, in principle, work as a spin filter and could be used for spin injection.

Figure 9 shows the position of the lowest transition threshold (sublevel) E_1 in the middle of a constriction with the same parameters as in previous figure. This graph should be compared with the conjecture of Reilly et al. shown in Figure 7. The LSDA results evidently confirm the assumption of a smooth, more or less linear opening of the spin-gap as the electron density increases. At the same time Figure 9 shows clearly that the gap closes gradually on further increase of the electron density. Thus the phenomenological model of Reilly et al. [28] should be extended to include this obvious feature. We also note that the positions of E_1 drops relative to the maximum of the tunneling potential. This is expected as the channel gets wider with increasing number of electrons due to the Coulomb interactions (Hartree term in Eqs. (14)).

It is an interesting question if the onset of magnetization and the opening of an energy gap will eventually become abrupt as a wire is made exceedingly long, as suggested in Ref. [25] and discussed in the section about ideal wires and interactions. Experimentally such a test might be hard, however, because of the sensitivity of long wires to impurities and imperfections. Accidental local constrictions (dents) may play a dominant role [58] and may hide an underlying long-wire physics.

The general features of Figures 8 and 9 obviously differ from the abrupt onset of polarization reported by Graham et al. [55]. These puzzling results needs further modeling to make sure that one indeed refers to the correct device characteristics.

8. Summary and concluding remarks

With focus on electron transport and dimensional crossover, we have outlined how modern semiconductor device technology, in addition to its vast impact on engineering applications, has opened new frontiers for fundamental research in condensed matter physics. Techniques to create tunable low-dimensional electron gas systems have matured and today high-mobility systems are fabricated routinely. We have seen how the ideas of the special GaAs-FET in Section 3 for studies of three to two dimensional crossover has developed

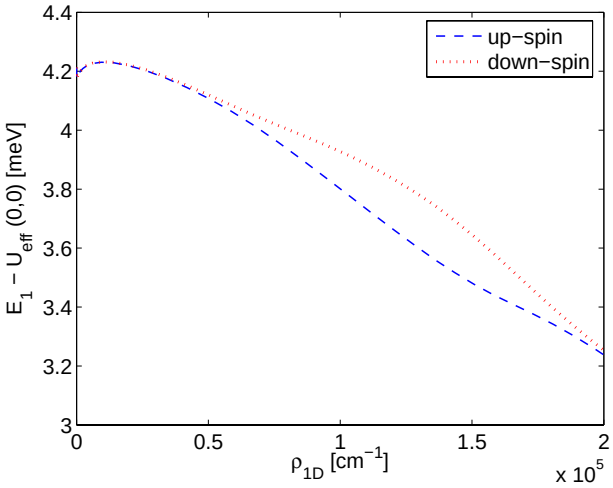

Figure 9. The energy difference between the lowest subband and the effective potential in the middle of the channel, as a function of the one-dimensional electron density, in channel with lithographic length 250 nm and width 80 nm. (From Ref. [50].)

into possibilities to tune 2D into 1D and thereby the emergence of quasi-1D ballistic electron gas devices. In particular, quantized conductance in QPCs and wires is a profound feature of quasi-1D electric transport. While the quantized steps are well understood, the mechanism behind the 0.7 conduction anomaly and its high B-field analogs are still debated.

Because of the sensitivity of transport data to the details of the potential landscape we have stressed the importance of including realistic device geometry and effects of leads/reservoirs in the modeling in order to make correct contact with experiments. For example, simple models suggest that the ground state of the interacting electrons may be ferro- or anti-ferromagnetic, a spin-density wave state, a Wigner lattice, a peculiar "zig-zag" structure etc. Using the local spin-density approximation (LSDA) simulations for realistic GaAs/AlGaAs split-gate devices have so far resulted in spontaneous ferromagnetic order within the conducting constriction. Further work, experimentally as well as theoretically, would be interesting to explore possible magnetization features of other geometries and type of devices. Much work also remains to model and analyze, for example, non-equilibrium transport data at finite source-drain voltages and the detailed spin-ordering features of the 0.7 analogs at Zeeman crossings of spin subbands.

LSDA is successful in predicting the existence of local magnetization induced by exchange and Coulomb interactions among the electrons. On the other hand, it fails to predict Kondo-like behavior and the ZBA. Effectively LSDA is a mean-field approach for the different occupied one-electron orbitals. The total wave function is a single determinant, which means that it cannot describe, for example, multi-configurational spin eigenstates. Therefore the LSDA modeling, as described above, concerns primarily the physics outside the "Kondo" regime, i.e., processes that rule above the "Kondo" temperature. Obviously spin polarization is an important mechanism in that regime, which is equally exciting as the "Kondo-like" mechanism because it may be used for spin injection and spin filtering.

Finally, much work remains before the "Kondo-like" or ZBA behavior will be well understood. Experimentally ZBA has been studied in detail only for short wires. Thus it would be of interest to have systematic studies also for long wires. Other aspects of ZBA concern the analog structures. As Graham et al. [55] remark that zero bias ZBA in the conduction has not been observed anywhere in the region of Zeeman crossings at high magnetic field B, although one observes structures enhanced in conductance by almost e^2/h, i.e., the 0.7 analogs. They deduce that the "Kondo-like" physics is not the cause of this enhancement and resultant analogs. Therefore they suggest that although the Kondo physics may well occur at $B = 0$, it is not the root of the 0.7 structure, but it may enhance its conductance. It is intriguing that ZBA has also been observed recently for the 2D electron gas [59] and may thus be of much more generic nature. Evidently much exciting modeling remains to be done in this context.

Acknowledgments

I wish to congratulate Professor Mehmet Tomak warmly on his 60th anniversary and also to thank him for scientific interactions and friendship since our initial work together back in the eighties on dimensional transitions and multi-subband transport. Furthermore I wish to thank Docent Irina Yakimenko for discussions and comments when preparing this article and Professor Sir Michael Pepper for communicating the results in Ref. [14] prior to publication.

Note added in proof:

There are recent important developments of the 0.7 structure. For example, shot-noise signatures of a QPC confirm density-dependent level splitting:
L. DiCarlo, Y. Zhang, D.T. McClure, D.J. Reilly, C.M. Marcus, L.N. Pfeiffer, and K.W. West, *Phys. Rev. Lett.,* **97**, (2006), 036810.

Quatum thermal conductance show anomalous features associated with the 0.7 structure:
O. Chiatti. J.T. Nicholls, Y.Y. Proskuryakov, N. Lumpkin, I. Farrer, and D.A. Ritchie, *Phys. Rev. Lett.,* **97**, (2006), 056601.

References

[1] M. Tomak, B. E. Sernelius, and K.-F. Berggren, *Phys. Rev. B*, **30**, (1984), 1016.

[2] B. E. Sernelius, K.-F. Berggren, M. Tomak, and C. McFadden, *J. Phys. C: Solid State Phys.*, **18**, (1985), 225.

[3] M. Taş and M. Tomak, *Phys. Rev. B*, **67**, (2003), 235314.

[4] M. Taş and M. Tomak, *Phys. Rev. B*, **70**, (2004), 235305.

[5] K.-F. Berggren and M. Pepper, *Physics World*, **10**, (2002), 37.

[6] M. I Elinson, V. A. Volkov, V. N. Lutskii, and T. N. Pinsker, *Thin Solid Films* , **12**, (1972), 383.

[7] Yu. F. Ogrin, V. N. Lutskii, and M. I Elinson, *JETP Lett.*, **3**, (1966), 71.

[8] D. A. Poole, M. Pepper, K.-F. Berggren, G. Hill, and H. W. Myron, *J. Phys. C: Solid State Phys.*, **15**, (1982), L21.

[9] D. J. Newson, K.-F. Berggren, M. Pepper, H. W. Myron, D. J. Davies, and E. G. Scott, *J. Phys. C: Solid State Phys.*, **19**, (1986), L403.

[10] T. J. Thornton, M. Pepper, H. Ahmed, D. Andrews, and G. J. Davies, *Phys. Rev. Lett.*, **56**, (1986), 1198.

[11] A. Kristiansen, H. Bruus, A. E. Hansen, J. B. Jensen, P. E. Lindelof, C. J Markmann, J. Nygaard, C. B. Sørensen, F. Beuscher, A. Forchel, and M. Michel, *Phys. Rev. B*, **62**, (2000), 10950.

[12] R. de Piciotto, L. N. Pfeiffer, K. W. Baldwin, and K. W. West, *Phys. Rev. B.*, **72**, (2005), 033319.

[13] R. Crook, A.C. Graham, C.G. Smith, I. Farrer, H.E. Beere , and D.A. Ritchie, *Nature*, **424**, (2003), 751.

[14] R. Crook, J. Prance, K.J. Thomas, S.J. Chorley, I. Farrer, D.A. Ritchie, M. Pepper and C.G. Smith, *Science*, **312**, (2006), 1359.

[15] A. A. Starikov, I. I. Yakimenko, and K.-F. Berggren, *Phys. Rev. B*, **67**, (2003), 235319.

[16] D. A. Wharam, T. J. Thornton, R. Newbury, M. Pepper, H. Ritchie , and G. A. C Jones, *J. Phys. C: Solid State Phys.*, **21**, (1988), L209.

[17] B. J. van Wees, H. van Houten, C. W. J. Beenakker, J. G. Williamson, L. P. Kouwenhoven, D. van der Marel, C. T. Foxton, and G. J. Davies, *Phys. Rev. Lett.*, **60**, (1988), 848.

[18] K. J. Thomas, J. T. Nicholls, N. J. Appleyard, M. Y. Simmons, M. Pepper, D. R. Mace, W. R. Tribe and D. A. Richie, *Phys. Rev. B.*, **58**, (1998), 4846.

[19] K. J. Thomas, J. T. Nicholls, M. Y. Simmons, M. Pepper, D. R. Mace, and D. A. Richie, *Phys. Rev. Lett.*, **77**, (1996), 135.

[20] K. S. Pyshkin, C. J. B. Ford, M. Pepper, E. H. Linfield, and D. A. Ritchie, *Phys. Rev. B*, **62**, (2000), 15842.

[21] R. Wirtz, R. Newbury, J. T. Nicholls, W. R. Tribe, M. Y. Simmons, and M. Pepper, *Phys. Rev. B*, **65**, (2002), 233316.

[22] D. J. Reilly, G. R. Facer, A. S. Dzurak, B. E. Kane, R. G. Clark, P. J. Stiles, A. R. Hamilton, J. L. O'Brien, N. E. Lumpkin, L. N. Pfeiffer, and K. W. West, *Phys. Rev. B*, **63**, (2001), R121311.

[23] R. Fitzgerald, *Phys. Today*, **55**, (2002), 21.

[24] J. R. Minkel, *Phys. Rev. Focus*, **10**, (2002), 24.

[25] C.-K. Wang and K.-F. Berggren, *Phys. Rev. B*, **54**, (1996), R14257.

[26] K.-F. Berggren, P. Jaksch, and I. Yakimenko, *Phys. Rev. B*, **71**, (2005), 115303.

[27] A. C. Graham, K. J. Thomas, M. Pepper, N. R. Cooper, M. Y. Simmons, and D. A. Ritchie, *Phys. Rev. Lett*, **91**, (2003), 136404.

[28] D. J. Reilly, T. M. Buchler, J. L. O'Brian, A. R. Hamilton, A. S. Dzurak, R. G. Clark, B. E. Kane, L. N. Pfeiffer, and K. W. West, *Phys. Rev. Lett.*, **89**, (2002), 246801.

[29] D. J. Reilly, *Phys. Rev. B*, **72**, (2005), 03309.

[30] D. J. Reilly, Y. Zhang, and L. DiCarlo, *Physica E Proc. EPS-16*, (2005).

[31] M. Taş, *PhD Thesis, The Middle East Technical University, Ankara, Turkey,* (2004).

[32] L. Calmels and A. Gold, *Europhys. Lett.*, **39**, (1997), 539.

[33] F. Malet, M. Pi, M. Barranco, and E. Lipparini, *Phys. Rev. B,* **72**, (2006). 205326.

[34] E. Lieb and D. Mattis, *Phys. Rev.*, **125**, (1962), 164.

[35] S. M. Reimann, M. Koskinen, and M. Manninen, *Phys. Rev. B*, **59**, (1999), 1613.

[36] S. M. Reimann and M. Manninen, *Rev. Mod. Phys*, **74**, (2002), 1283.

[37] A. D. Klironomos, J. S. Meyer, and K. A. Matveev, *cond-mat/0507387*, (2005).

[38] A. D. Klironomos, R. R. Ramazashvili, and K. A. Matveev, *Phys. Rev. B*, **72**, (2005), 195343.

[39] D. L. Maslov and M. Stone, *Phys. Rev. B*, **52**, (1995), R5539.

[40] M. Büttiker, *Phys. Rev. B*, **41**, (1990), 7906.

[41] L. Martín-Moreno, J. T. Nicholls, N. K. Patel, and M. Pepper, *J. Phys. C: Condens. Matter*, **4**, (1992), 1323.

[42] P. Jaksch, K.-F. Berggren, and I. I. Yakimenko, *Nanotechnology*, **16**, (2005), 1924.

[43] C.-K. Wang and K.-F. Berggren, *Phys. Rev. B*, **54**, (1998), 14257.

[44] K.-F. Berggren and I. I. Yakimenko, *Phys. Rev. B*, **66**, (2002), 085323.

[45] Y. Meir, K. Hirose, and N. S. Wingreen, *Phys. Rev. Lett.*, **89**, (2002), 196802.

[46] K. Hirose, Y. Meir, and N. S. Wingreen, *Phys. Rev. Lett.*, **90**, (2003), 026804.

[47] P. Havu, M. J. Puska, R. M. Nieminen, and V. Havu, *Phys. Rev. B*, **70**, (2004), 233308.

[48] P. S. Cornaglia, C. A. Balseiro, and M. Avignon, *Phys. Rev. B*, **71**, (2005), 024432.

[49] A. Ashok, R. Akis, D.Vasileska, and D. K. Ferry, *Molecular Simulation*, **31**, (2005), 797.

[50] P. Jaksch, I. I. Yakimenko, and K.-F. Berggren, *(in press)*, (2006).

[51] L. P. Rokhinson, L. N. Pfeiffer, and K. W. West, *Phys. Rev. Lett.,* **96**, (2006), 156602.

[52] S. M. Cronenwett, H. J. Lynch, D. Goldhaber-Gordon, L. P. Kouwenhoven, C. M. Marcus, K. Hirose, N. S. Wingren, and V. Umansky, *Phys. Rev. Lett.*, **88**, (2002), 226805.

[53] P. E. Lindelof, *Proceedings of SPIE*, **4415**, (2001), 77.

[54] P. S. Cornaglia and C. A. Balseiro, *Europhys. Lett*, **67**, (2004), 634.

[55] A. C. Graham, M. Pepper, M. Y. Simmons, and D. A. Ritchie, *Phys. Rev. B*, **72**, (2005), 193305.

[56] D. Schmelzer, *cond-mat/0211490,* (2002).

[57] K. A. Matveev, *Phys. Rev. B*, **70**, (2004), 245319.

[58] A. A. Starikov, I. I. Yakimenko, K.-F. Berggren, A. C. Graham, K. J. Thomas, M. Pepper, and M. Y. Simmons, *SPIE*, **5023**, (2002), 267.

[59] A. Ghosh, C. J. B. Ford, M. Pepper, H. E. Beere, and D. A. Ritchie, *Phys. Rev. Lett.*, **92**, (2004), 116601.